Design and Development of Hot Corrosion-Resistant Nickel-Base Single-Crystal Superalloys by the *d*-Electrons Alloy Design Theory: Part I. Characterization of the Phase Stability

J.S. ZHANG, Z.Q. HU, Y. MURATA, M. MORINAGA, and N. YUKAWA

As the first step to design and develop the new hot corrosion-resistant nickel-base single-crystal superalloys by the *d*-electrons alloy design theory (or the New PHACOMP), an evaluation of the phase stability of the modified hot corrosion-resistant IN738LC nickel-base superalloys (Ni-16Cr-9.5Al-4.0Ti-8.0-Co-0.55Nb-0.06Zr-0.05B-0.47C-(0~3)Ta-(0~3)W-(0~3)Mo (in atomic percent)) was conducted with the alloy design theory. The critical conditions for suppressing the precipitation of the brittle σ phase can be described by the electronic parameters $\overline{Mdt} \leq 0.991$ and $\overline{Md\gamma} \leq 0.93$ which can be applied to the *d*-electrons alloy design of hot corrosion resistant nickel-base superalloys with high Cr contents.

I. INTRODUCTION

THE progress in optimization of alloy compositions and innovation of the processing techniques has effectively improved the service temperature capabilities of the blades and vanes of gas turbine engines. The single-crystal blades developed in recent years are a good example. These blades have shown advantages in their properties such as higher strength at high temperatures, better resistance to fatigue and thermal fatigue, *etc*. They have been widely used in the high-performance aerial gas turbine engines. The efficiency and service life of the gas turbine engines have been improved markedly. A series of alloys with the compositions suitable for the single-crystal processing have been developed, *e.g.*, the PWA,[1] CMSX,[2] SRR,[3] TMS,[4] and TUT[5] series of alloys. The most recently developed single-crystal nickel-base superalloy TMS26 in Japan[6] is among the highest service-temperature single-crystal superalloys in the world, at present time, with a service temperature about 37 °C higher than that of the second generation high-performance single-crystal superalloys such as PWA1484. Unfortunately, in the development of single-crystal superalloys, only few efforts have been put on the development of the so-called "hot corrosion-resistant single-crystal superalloys" which will be the key materials for the blades and vanes of the long-term and high-performance marine and industrial gas turbines. The purpose of this study is to search for the proper alloy compositions of hot corrosion-resistant nickel-base superalloys with promising comprehensive properties under the guidance of the *d*-electrons alloy design theory (or New PHACOMP (*PHA*se *COMP*utation)). This method is a newly developed alloy design concept based on *DV-Xα* cluster calculations of electronic structure of transition metals.[7,8,9] Two calculated electronic parameters Md and Bo (*d*-orbital energy level and bond order of alloying transition metals) are employed as the controlling factors of the phase stability and properties. In the alloy design, the average values of Md and Bo are defined taking the compositional average as

$$\overline{Mdt} = \Sigma Xi(Md)i \quad [1]$$

$$\overline{Bot} = \Sigma Xi(Bo)i \quad [2]$$

where Xi, $(Md)i$, and $(Bo)i$ are the atomic fraction, Md and Bo values of element i in an alloy, respectively. Similarly, $\overline{Md\gamma}$ is denoted for the γ phase. The details for the applications of this alloy design method in the development of nickel-base superalloys have been published elsewhere.[5,10,11]

In this study, the most widely used hot corrosion-resistant nickel-base superalloy IN738LC was taken as the reference alloy to develop a new hot corrosion-resistant single-crystal nickel-base superalloy with equivalent hot corrosion resistance but with markedly improved high-temperature mechanical properties. This study is composed of three parts. In the first part, the critical electronic parameters controlling the phase stability of hot corrosion-resistant alloy systems with high Cr contents (modified IN738LC alloy series) were determined. In the second part, the effects of refractory metals (Ti, Ta, and Nb) on various properties, except for the mechanical properties, were studied systematically, and the compositional regions with promising comprehensive properties were determined for the final single-crystal growth and mechanical property characterizations. In the third part, the most promising alloy compositions were selected for single-crystal growth and mechanical property evaluation, and finally, the optimum alloy composition, with the comprehensive properties satisfying the alloy design goals, was determined. The results of the first part are reported in this article as the basis of the whole study.

J.S. ZHANG, Associate Professor, formerly with the Institute of Metal Research, Academia Sinica, Shenyang 110015, China, is with the Department of Materials Science and Engineering, Beijing University of Science and Technology, Beijing 100083, China. Z.Q. HU, Professor, is with the Institute of Metal Research, Academia Sinica, Shenyang 110015, China. Y. MURATA, Associate Professor, and M. MORINAGA and N. YUKAWA, Professors, are with the Department of Production Systems Engineering, Toyohashi University of Technology, Toyohashi 441, Japan.

Manuscript submitted June 8, 1992.

Table I. Compositions of the Alloys (Atomic Percent)

Alloy	Cr	Co	Zr	Nb	Ti	Al	Ta	Mo	W	C	B	Ni	Ta/(W + Mo)	W/Mo	$\overline{Mdt}$	$\overline{Bot}$
Z1	16.0	8.0	0.06	0.55	4.0	9.5	1.08	0.27	0.27	0.47	0.05	59.57	2/1	1/1	0.986	0.696
Z21	16.0	8.0	0.06	0.55	4.0	9.5	1.33	0.33	0.33	0.47	0.05	59.37	2/1	1/1	0.991	0.701
Z2	16.0	8.0	0.06	0.55	4.0	9.5	1.58	0.40	0.40	0.47	0.05	58.99	2/1	1/1	0.996	0.705
Z3	16.0	8.0	0.06	0.55	4.0	9.5	2.09	0.52	0.52	0.47	0.05	58.23	2/1	1/1	1.010	0.714
Z4	16.0	8.0	0.06	0.55	4.0	9.5	0.88	0.44	0.44	0.47	0.05	59.62	1/1	1/1	0.986	0.698
Z22	16.0	8.0	0.06	0.55	4.0	9.5	1.08	0.54	0.54	0.47	0.05	59.20	1/1	1/1	0.991	0.703
Z5	16.0	8.0	0.06	0.55	4.0	9.5	1.29	0.65	0.65	0.47	0.05	58.79	1/1	1/1	0.996	0.708
Z6	16.0	8.0	0.06	0.55	4.0	9.5	1.71	0.85	0.85	0.47	0.05	57.96	1/1	1/1	1.010	0.717
Z7	16.0	8.0	0.06	0.55	4.0	9.5	0.74	0.56	0.56	0.47	0.05	59.52	2/3	1/1	0.986	0.699
Z23	16.0	8.0	0.06	0.55	4.0	9.5	0.92	0.69	0.69	0.47	0.05	59.08	2/3	1/1	0.991	0.704
Z8	16.0	8.0	0.06	0.55	4.0	9.5	1.09	0.82	0.82	0.47	0.05	58.65	2/3	1/1	0.996	0.709
Z9	16.0	8.0	0.06	0.55	4.0	9.5	1.44	1.08	1.08	0.47	0.05	57.77	2/3	1/1	1.010	0.720
Z10	16.0	8.0	0.06	0.55	4.0	9.5	0.64	0.64	0.64	0.47	0.05	59.45	1/2	1/1	0.986	0.700
Z24	16.0	8.0	0.06	0.55	4.0	9.5	0.79	0.79	0.79	0.47	0.05	59.00	1/2	1/1	0.991	0.705
Z11	16.0	8.0	0.06	0.55	4.0	9.5	0.94	0.94	0.94	0.47	0.05	58.54	1/2	1/1	0.996	0.710
Z12	16.0	8.0	0.06	0.55	4.0	9.5	1.24	1.24	1.24	0.47	0.05	57.64	1/2	1/1	1.010	0.721
IN738	17.5	8.2	0.06	0.55	4.0	7.1	0.54	1.01	0.81	0.47	0.05	60.06			0.976	0.722

II. EXPERIMENTAL

Based on the compositions of IN738LC, the alloy system Ni-16Cr-9.5Al-4.0Ti-8.0Co-0.55Nb-0.06Zr-0.05B-0.47C-(0~3)Ta-(0~3)W-(0~3)Mo (in atomic percent) was selected for investigation. The compositions of the alloys studied are given in Table I, in which $\overline{Mdt}$ and $\overline{Bot}$ values were calculated from Eqs. [1] and [2]. The composition of the reference alloy IN738LC is also included in the table. The Md and Bo values of the alloying elements used in the calculations are listed in Table II.

For comparison, the conventional PHACOMP parameter $\overline{Nv}$ was calculated using the compositions of the γ phase determined in this study. The $\overline{Nv}$ values were calculated with the method introduced by Decker,[17] as

$$\overline{Nv} = 0.66Ni + 1.71Co + 4.66(Cr + Mo + W) + 5.66(Nb + Ta) + 6.66Ti + 7.66Al$$

where the compositions are in atomic percent.

High-purity metals were used to make the experimental alloys. Samples (about 10 g in weight for each) with button sizes were made by a tri-arc furnace in a purified argon atmosphere. The furnace electrodes were made of tungsten and water-cooled. Alloy melting was conducted in a water-cooled copper crucible with a melting voltage of 80 V and current of 40 A for each electrode. The molten samples rotated within the crucible because of the electromagnetic action of the three electrodes and the surface tension of the melt. This was beneficial to compositional homogenization. Each button was turned over and remelted five times to achieve homogeneity and complete dissolution of refractory metals. Weight losses were always less than 1 pct after the five remelts.

Table II. List of the Values of Md and Bo

Element	Md	Bo	Element	Md	Bo
Ti	2.271	1.098	Zr	2.944	1.479
V	1.543	1.141	4d Nb	2.117	1.594
Cr	1.142	1.278	Mo	1.550	1.611
Mn	0.957	1.001	Hf	3.020	1.518
3d Fc	0.858	0.857	5d Ta	2.224	1.670
Co	0.777	0.697	W	1.655	1.730
Ni	0.717	0.514	Al	1.900	0.533
Cu	0.615	0.272	Si	1.900	0.589

Solidification behavior of the alloys studied was examined by differential thermal analysis (DTA). The apparatus used was DT-1500H. All measurements were made under a flowing purified argon atmosphere to a temperature of 1450 °C at a constant heating rate (5 °C/min), and then cooled at the same rate, through the solidification temperature range. The samples (about 200 mg in weight) with the sizes of 3.5 mm in diameter and 2.5 mm in height used in DTA measurements were taken from the center part of the buttons. The reference material is a high-purity Al_2O_3 powder. The melting temperature of pure gold (Tm = 1063 °C) was regularly measured on the same instrument to correct the measured temperatures. Reaction temperatures were determined by finding the temperature at which the DTA curve deviated from the local baseline.[13] Reaction temperatures were determined from cooling curves, except for the solidus temperatures.

After the full heat treatment (1120 °C/2 h/AC + 850 °C/24 h/AC), the samples were aged at 900 °C for 500 hours and water quenched, then examined by optical and scanning electron microscopy (SEM) to determine the phase stability boundary. To get the compositions of γ and γ' phases accurately by an electron probe microanalyzer (EPMA), a special procedure was followed to get the equilibrium large γ and γ' recrystallization structures: solution treatment → cold working → holding at 1100 °C for 72 hours → cooling slowly at a rate of 1 °C/min to 900 °C → holding at 900 °C for 500 hours → water quenching.

The compositions of the phases in the alloys were measured with a Hitachi X-650 electron probe microanalyzer. The eutectic ($\gamma + \gamma'$) volume fraction in the samples after DTA was determined by an imaging analysis equipment.

Metallography was performed on both as-cast and heat-treated specimens. Prior to examination *via* optical and

SEM, the polished specimens were etched in a solution of $CuSO_4$(20 g) + HCl (100 ml) + H_2O (80 ml) + H_2SO_4(5 ml).

III. EXPERIMENTAL RESULTS

Table III shows the results of the DTA analysis of the solidification behavior of the experimental alloys, including the eutectic ($\gamma + \gamma'$) volume fraction in the samples after DTA. Figure 1 shows some typical DTA curves. The following reactions occurred during the solidification process: $P_0(\gamma + \gamma' \rightarrow L)$, $P_1(L \rightarrow \gamma)$, $P_2(L \rightarrow \gamma + \gamma')$, $P_3(\gamma \rightarrow \gamma')$, and $P_4(L \rightarrow$ MC carbide). Compared with IN738LC alloy, the experimental alloys showed the same solidification path. Note that in the experimental alloys, the γ' solvus temperatures were increased obviously. This could be related to the higher Al and Ta contents in the alloys and could be beneficial to the increase of the high-temperature mechanical properties. Figure 2 shows the typical microstructures in the specimens after DTA. All the alloys show similar as-cast structures with γ and γ' phases in the dendrite arms and eutectic ($\gamma + \gamma'$) pools in the interdendritic regions. In the compositional range studied, the melting range ($\Delta T = P_1 - P_0$) and eutectic ($\gamma + \gamma'$) volume fraction decreased as the ratio of Ta/(W + Mo) increased (Figure 3), which indicates that the Ta/(W + Mo) ratio was also an important factor controlling the phase stability and single-crystal castability (related to ΔT) of the alloy system studied.

To get the important parameter $\overline{Md\gamma}$ for the characterization of phase stability of nickel-base superalloys, the compositions of γ phase had to be measured first. The compositions of γ and γ' phases were measured by EPMA with the specially treated specimens with coarsened γ and γ' recrystallization structures (Figure 4). The results are listed in Table IV including the calculated $\overline{Md\gamma}$ values. Metallographic observations on the 16 alloys selected from the alloy system studied after long-term aging at 900 °C for 500 hours (Figure 5) showed that the critical condition for suppressing the precipitation of harmful brittle TCP phase (in this case, σ phase) could be expressed with the electronic parameter as $\overline{Md\gamma} \leq 0.93$, which becomes the phase stability boundary condition for suppressing σ phase and is the same as that for other nickel-base superalloys with low Cr contents.[15] The partitioning ratios (atomic ratio between γ' and γ phases) of Al, Ti, Ta, and Nb which can be easily calculated from the data shown in Table IV were always greater than unity, which means that these elements mainly enter the γ' phase, or they are the γ' phase forming elements.

Figure 6 summarizes the results of the previous phase stability analysis. It can be seen that in addition to the critical parameter $\overline{Md\gamma} \leq 0.93$, another parameter $\overline{Mdt} \leq 0.991$ could also be used as a criterion controlling the phase stability of the alloy system studied. When $\overline{Mdt}$ was over 0.991, the σ phase began to precipitate.

IV. DISCUSSION

The compositional features of two kinds of nickel-base superalloys (single-crystal and hot corrosion-resistant alloys) reported in the literature are summarized in

Table III. DTA Results (Reaction Temperatures in °C) and Eutectic ($\gamma + \gamma'$) Volume Fractions of Designed Alloys

Alloy	P_0	P_1	P_2	P_3	P_4	ΔT	($\gamma + \gamma'$) vol pct
IN738LC	1282	1346	1230	1166	1298	64	2.194
Z1	1270	1326	1230	1209	1301	56	1.248
Z2	1243	1325	1214	1196	1287	58	2.525
Z3	1246	1310	1226	1208	1292	64	3.695
Z4	1270	1331	1229	1208	1304	61	1.546
Z5	1249	1325	1226	1200	1298	64	2.890
Z6	1270	1337	1232	1217	1304	67	4.016
Z7	1249	1316	1200	1200	1286	67	1.773
Z8	1257	1326	1232	1214	1304	69	3.717
Z9	1252	1322	1232	1211	1304	70	4.123
Z10	1264	1334	1226	1208	1292	70	2.000
Z11	1249	1320	1220	1190	1298	71	3.901
Z12	1249	1322	1232	1205	1295	73	4.863

P_0: $\gamma + \gamma' \rightarrow L$; P_1: $L \rightarrow \gamma$; P_2: $L \rightarrow \gamma + \gamma'$; P_3: $\gamma \rightarrow \gamma'$; P_4: $L \rightarrow$ MC carbide, and $\Delta T = P_1 - P_0$.

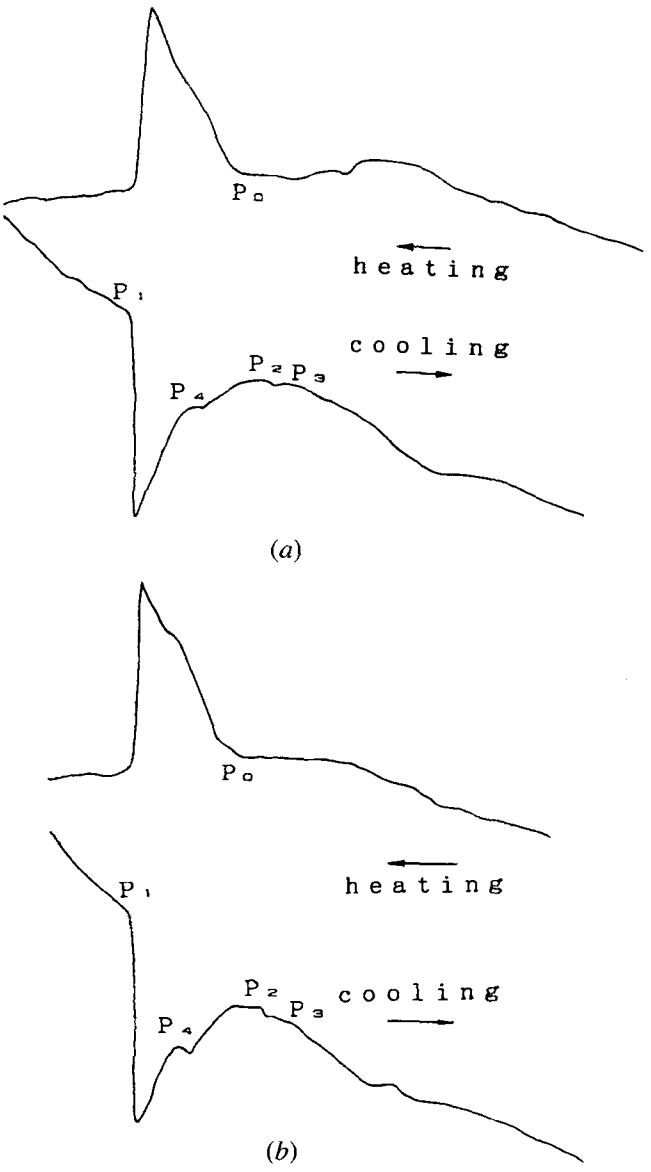

Fig. 1—Typical DTA curves. (*a*) IN738LC and (*b*) alloy Z10.

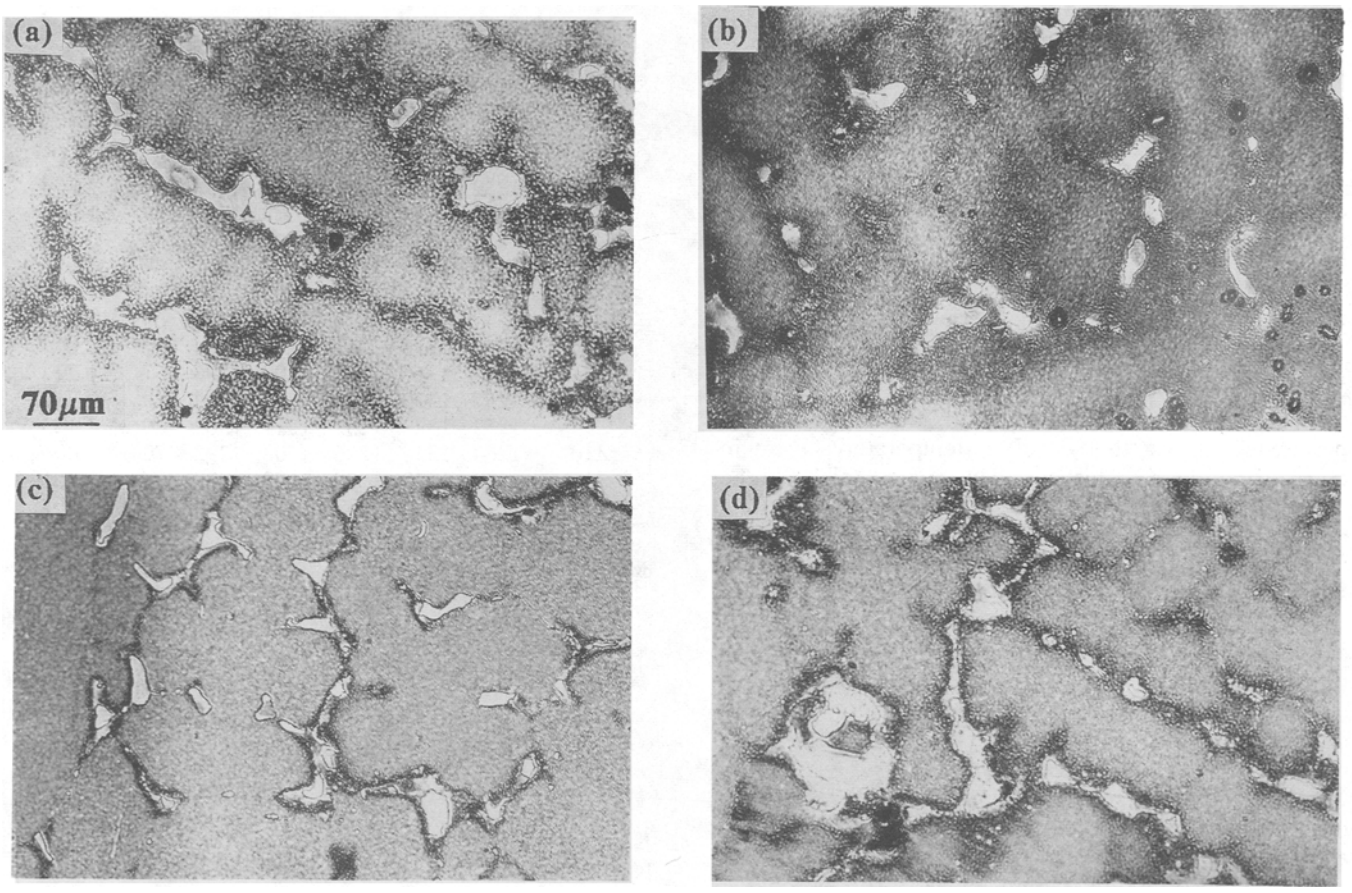

Fig. 2—Typical microstructures in the samples after DTA. (*a*) IN738LC ($\overline{Mdt}$ = 0.976), (*b*) alloy Z4 ($\overline{Mdt}$ = 0.986), (*c*) alloy Z2 ($\overline{Mdt}$ = 0.996), and (*d*) alloy Z9 (Mdt = 1.010).

Figure 7. Most of the high-performance single crystals contain a relatively low Cr content (usually less than 10 at. pct). It is well known that Cr is the most important and effective alloying addition for the hot corrosion resistance in superalloys.[12] The alloys with low Cr content usually show poor hot corrosion resistance. Unfortunately, this is the case for most of the single-crystal superalloys developed until now. In the hot corrosion-resistant polycrystalline alloys, the Cr contents are usually higher than 14 at. pct, but the contents of Al and other refractory alloying elements which are important for the high-temperature mechanical properties are relatively low. To get the optimum comprehensive properties with desired balance between hot corrosion resistance and high-temperature mechanical property, based on the compositions of IN738LC, the high content of Cr was maintained and the Al content was properly increased in the alloy design consideration. According to the *d*-electrons alloy design theory, the principle for selecting alloying elements is that the Bo value should be as high as possible for improving solution strengthening while the Md value should be relatively low for better phase stability. From Table II, the 5d elements W and Ta, and the 4d element Mo show the highest Bo values in order. They are the desirable alloying elements for improving high-temperature strength of the nickel-base alloys. Therefore, the effects of these three elements on the phase stability of the high Cr-content alloy system were studied systematically in this study, as shown in Figure 6.

The results of phase stability characterization show that boundary conditions of phase stability are almost the same as in the alloy systems with lower Cr contents, *i.e.*, $\overline{Mdt}$ = 0.991 and $\overline{Md\gamma}$ = 0.93 (Figure 6), only with a slightly higher $\overline{Mdt}$ value.[10,11] These results indicate that through proper compositional adjustment (controlled by the electronic parameters $\overline{Mdt}$ and $\overline{Bot}$), promising results could be achieved with the alloy design process. It means that in the alloy systems with high Cr contents, the amount of Al and refractory elements can be increased properly to improve the high-temperature mechanical properties. At the same time, the Cr contents can be kept at a high level to maintain the hot corrosion resistance. As shown in Table I, the reference alloy IN738LC shows lower $\overline{Mdt}$ but higher $\overline{Bot}$ values which allows an increase in the $\overline{Mdt}$ to the critical value that is controlling the phase stability of the alloy system as determined in this study. In this way, the mechanical properties of the alloys could be improved by proper compositional adjustment because if the $\overline{Mdt}$ value is to

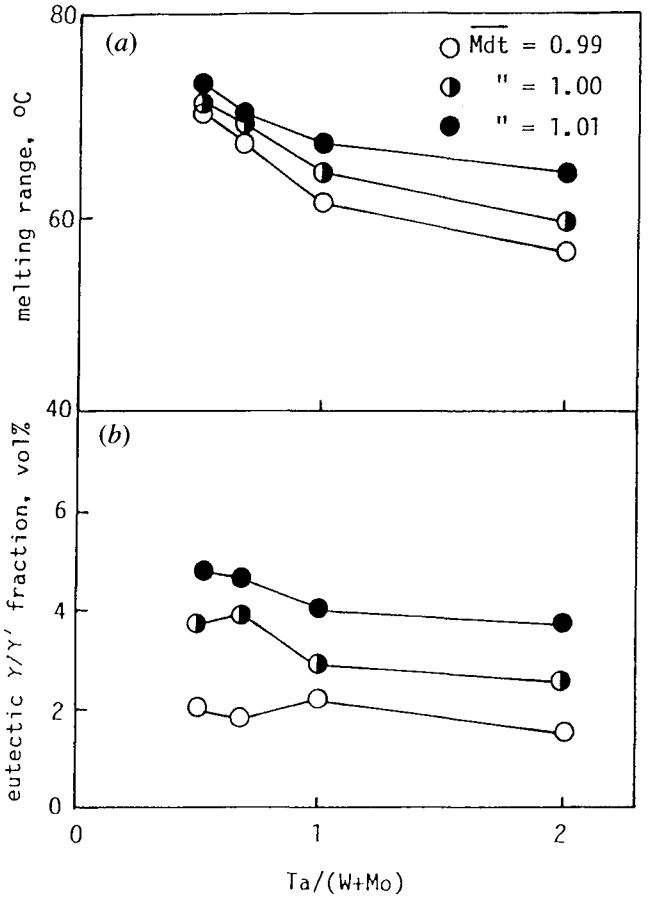

Fig. 3—Dependence of (*a*) melting range (ΔT) and (*b*) eutectic ($\gamma + \gamma'$) volume fraction of the experimental alloys upon the Ta/(W + Mo) ratio.

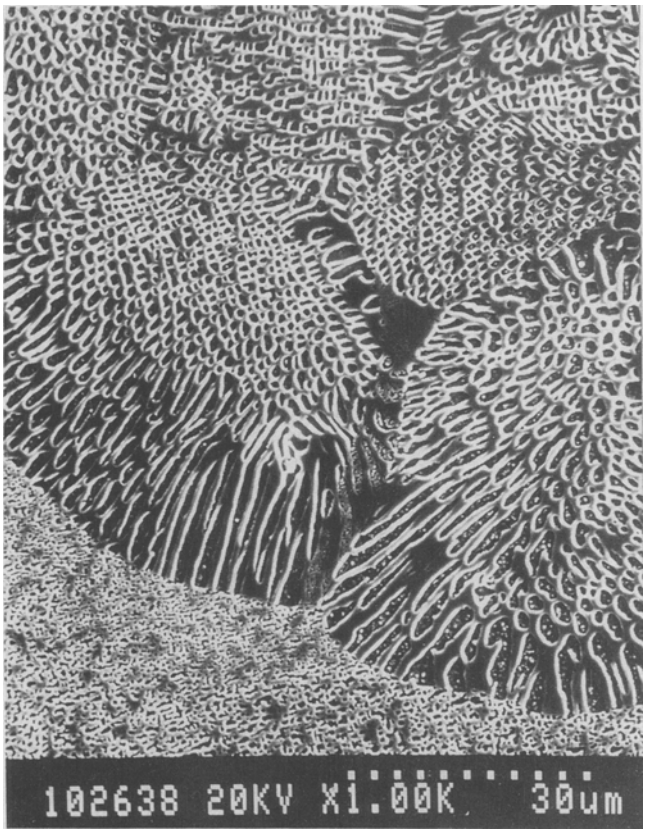

Fig. 4—The coarsening equilibrium γ and γ' recrystallization structures in the samples employed for the accurate EPMA analysis.

be increased, more alloying elements could be added in the alloys.

By comparing the parameters used in the new and the conventional PHACOMP methods ($\overline{Mdt}$, $\overline{Md\gamma}$, and $\overline{Nv}$, as shown in Tables I and IV), it can be seen that the new PHACOMP method can give more satisfactory boundary conditions ($\overline{Mdt}$ = 0.991 or $Md\gamma$ = 0.93) controlling the phase stability, while the $\overline{Nv}$ PHACOMP method cannot give definitive boundary conditions. As shown in Table IV, at the boundary separating the σ-free and σ-prone regions determined by the $\overline{Md}$ parameters (as shown by the dotted line in Figure 6), $\overline{Nv}$ values scattered between 2.182 and 2.208. Although the $\overline{Nv}$ values of the alloys studied were lower than the critical value suggested by Decker[17] (Nv = 2.26 ~ 2.41), σ phase was observed in many of the alloys. This indicates that the $\overline{Nv}$ method is inadequate for this alloy design process compared to the $\overline{Md}$ method.

It was found that when the quantity of eutectic ($\gamma + \gamma'$) in the microstructure of an alloy is lower than a critical value (≤2 vol pct in the samples after DTA), such nonequilibrium coarsening structures could be eliminated by solution treatment.[5] In the alloy system studied, the critical condition was determined as $\overline{Mdt} \leq 0.991$.

As can be seen from Figure 6, two lines representing the phase stability boundary ($\overline{Md\gamma}$ = 0.93) and boundary of removing the eutectic ($\gamma + \gamma'$) through the post solution treatment ($\overline{Mdt}$ = 0.991) were actually overlapped, and may be considered practically as one line. Therefore, the two critical values are equivalent in representing the phase stability. We can employ $\overline{Mdt}$ instead of $\overline{Md\gamma}$ in alloy design. This will be an easier and more convenient method for the alloy design process, because the $\overline{Mdt}$ value can be calculated directly from alloy compositions, while in the $\overline{Md\gamma}$ method, the γ phase compositions must be determined first by experiments.

The alloying elements Al, Ti, Ta, and Nb are the γ' forming elements and mainly partition to the γ' phase (Table IV), which is similar to other nickel-base superalloys with low Cr contents.[14,15] Because γ' is the main strengthening phase in nickel-base superalloys, it will be the key factor determining the properties of an alloy, including mechanical and hot corrosion-resistant properties. To achieve the goals of the alloy design, *i.e.*, to develop new alloys with desired balance of the comprehensive properties, the effects of these elements in the alloy system should be studied systematically. Our efforts to achieve this goal are described in the second part of this study.[16]

From the results of the evaluation of phase stability of the modified IN738LC alloy system Ni-16Cr-9.5Al-4.0Ti-8.0Co-0.55Nb-0.06Zr-0.05B-0.47C-Ta-W-Mo (in atomic percent) by the *d*-electrons alloy design theory or the New PHACOMP, it has been proved that the phase stability boundary conditions (described by the electronic parameters $\overline{Mdt}$ and $\overline{Md\gamma}$) of the hot corrosion-resistant alloy

Table IV. Compositions of γ and γ' and the $\overline{Md\gamma}$ Values of the Designed Alloys (Measured by EPMA)

		Al	Ti	Cr	Co	Zr	Nb	Mo	Ta	W	Ni	$\overline{Md\ \gamma}$	$\overline{Nv}$
Z1	γ	5.25	2.05	19.02	14.57	0.069	0.26	0.81	0.54	0.63	55.78	0.9192	2.155
	γ'	12.42	6.53	3.91	6.05	0.035	0.62	0.13	2.75	0.21	68.26		
Z21	γ	4.06	2.00	20.92	14.84	0.074	0.31	0.97	0.69	0.86	55.77	0.9300	2.183
	γ'	12.65	6.38	3.92	4.81	0.033	0.67	0.17	3.25	0.26	67.93		
Z2	γ	4.53	2.01	20.30	14.84	0.073	0.24	1.26	0.79	0.98	55.81	0.9396	2.212
	γ'	12.86	5.50	3.75	5.06	0.031	0.76	0.23	3.77	0.34	68.01		
Z3	γ	5.00	2.05	19.02	14.21	0.076	0.27	1.56	1.09	1.42	55.79	0.9491	2.233
	γ'	13.41	5.53	2.58	3.85	0.038	0.80	0.35	4.93	0.48	67.94		
Z4	γ	5.03	2.04	19.32	14.80	0.069	0.28	0.86	0.44	0.72	55.84	0.9198	2.158
	γ'	13.21	6.53	3.96	5.04	0.036	0.71	0.18	2.17	0.25	67.90		
Z22	γ	5.82	2.00	19.04	13.66	0.076	0.31	1.21	0.54	0.81	55.45	0.9301	2.208
	γ'	12.87	6.52	3.76	5.05	0.034	0.68	0.21	2.67	0.28	67.88		
Z5	γ	4.32	2.01	20.91	14.54	0.075	0.33	1.47	0.65	0.95	55.45	0.9392	2.222
	γ'	13.23	5.75	3.92	4.81	0.043	0.74	0.29	3.14	0.19	67.84		
Z6	γ	4.79	2.05	19.32	14.82	0.070	0.26	1.96	0.86	1.28	55.50	0.9495	2.238
	γ'	13.45	5.57	2.54	4.82	0.038	0.70	0.43	4.52	0.38	67.50		
Z7	γ	4.04	2.03	20.56	14.84	0.072	0.34	1.14	0.37	0.72	55.76	0.9199	2.151
	γ'	12.84	6.35	3.92	5.01	0.031	0.65	0.29	1.91	0.23	68.75		
Z23	γ	4.31	2.08	20.56	14.80	0.073	0.31	1.25	0.46	0.91	55.46	0.9299	2.190
	γ'	13.06	6.51	3.94	5.03	0.032	0.74	0.32	2.31	0.28	67.72		
Z8	γ	4.06	2.00	21.20	14.51	0.068	0.31	1.58	0.55	0.98	55.83	0.9392	2.217
	γ'	13.27	5.51	2.93	4.84	0.035	0.69	0.37	3.99	0.32	68.00		
Z9	γ	5.01	2.04	19.05	14.58	0.077	0.34	2.03	0.72	1.35	55.44	0.9491	2.240
	γ'	13.44	5.53	3.10	4.81	0.031	0.66	0.45	3.47	0.39	68.08		
Z10	γ	5.25	2.04	19.05	14.23	0.069	0.34	0.96	0.32	0.82	55.85	0.9194	2.158
	γ'	12.81	6.57	3.95	5.00	0.034	0.68	0.15	1.60	0.26	69.02		
Z24	γ	3.80	2.06	21.17	14.83	0.075	0.30	1.42	0.41	0.84	55.83	0.9299	2.182
	γ'	13.21	6.55	3.73	5.04	0.038	0.66	0.39	1.93	0.35	68.08		
Z11	γ	4.29	2.01	20.89	14.86	0.074	0.29	1.64	0.47	1.06	55.46	0.9406	2.225
	γ'	13.64	5.72	3.91	4.84	0.033	0.71	0.39	2.34	0.36	68.05		
Z12	γ	4.78	2.04	19.33	14.51	0.071	0.32	2.20	0.62	1.32	55.76	0.9490	2.236
	γ'	14.06	5.53	2.90	5.01	0.035	0.70	0.51	3.08	0.41	67.72		

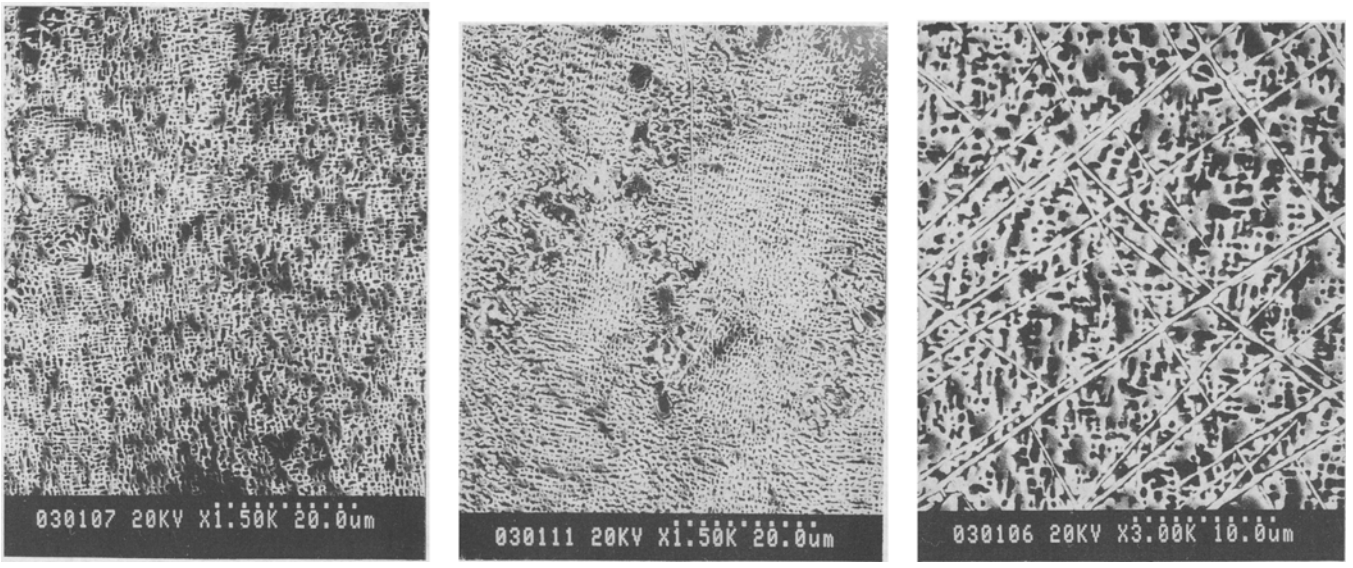

(*a*) (*b*) (*c*)

Fig. 5—Typical microstructures in the specimens after long-term aging at 900 °C for 500 h. (*a*) σ-free (Z21 with $\overline{Mdt}$ = 0.991) and (*b*) and (*c*) σ-prone (Z11 and Z3 with Mdt = 0.996 and 1.010, respectively).

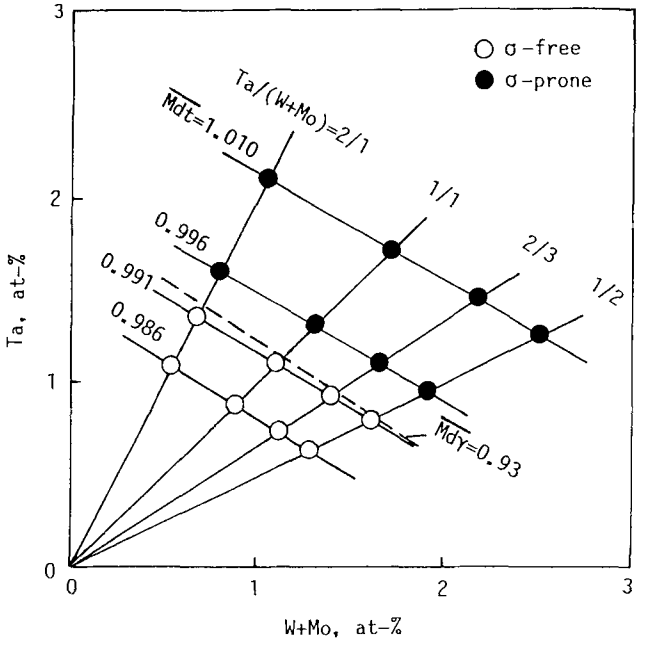

Fig. 6—Phase stability diagram for the alloy system Ni-16Cr-9.5Al-4.0Ti-8.0Co-0.55Nb-0.06Zr-0.05B-0.47C-Ta-W-Mo (in at. pct).

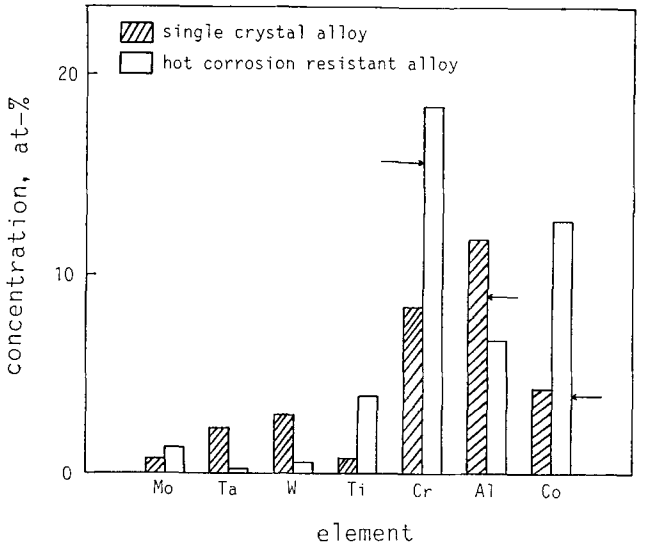

Fig. 7—Alloying features of two types of nickel—base superalloys (single-crystal and hot corrosion-resistant alloys) reported in the literature. The arrows indicate the positions of the designed alloys.

systems with high Cr contents is almost the same as those of the single-crystal superalloys with lower Cr and higher Al contents (typically, $\overline{Mdt} = 0.985$[15]). It indicates that through proper compositional adjustment (mainly the γ' forming elements Al, Ti, Ta, and Nb), the new high-performance hot corrosion-resistant single-crystal nickel-base superalloys can be developed. The direction of the next study was determined based on the previous results, *i.e.*, the effects of three refractory metals Ti, Ta, and Nb on the phase stability and other properties of the alloy system should be studied systematically to find the optimum alloy compositions and then develop the high-performance hot corrosion-resistant single-crystal superalloys. The results will be published in another article.[16]

V. CONCLUSIONS

1. The critical conditions for phase stability of the hot corrosion-resistant alloy system Ni-16Cr-9.5Al-4.0Ti-8.0Co-0.55Nb-0.06Zr-0.05B-0.47C-Ta-W-Mo (in atomic percent) can be described by the electronic parameters $\overline{Mdt} \leq 0.991$ and $\overline{Md\gamma} \leq 0.93$, which are similar to those for the alloy systems with lower Cr and higher Al contents.
2. The phase stability criteria of $\overline{Mdt}$ and $\overline{Md\gamma}$ are practically equivalent. Therefore, instead of using the $\overline{Md\gamma}$ parameter, the critical $\overline{Mdt}$ value can be used for the simpler and more convenient alloy design process.
3. In the compositional range studied, the melting range ΔT (determining the single-crystal castability) and eutectic ($\gamma + \gamma'$) volume fraction decrease with the $\overline{Ta}/(W + Mo)$ ratio, but increase with the $\overline{Mdt}$ values.
4. The alloying elements Al, Ti, Ta, and Nb mainly enter the γ' phase or they are the γ' forming elements in the alloy system studied.

ACKNOWLEDGMENT

The authors are grateful to Drs. H. Ezaki and K. Matsugi for their assistance in the study and helpful discussions on the results.

REFERENCES

1. A.D. Cetel and D.N. Duhl: *Superalloys 1988, Proc. Int. Symp. on Superalloys*, Seven Springs, Champion, PA, Sept. 1988, D.N. Duhl, G. Maurer, S. Antolovich, C. Lund, and S. Reichman, eds., TMS, Warrendale, PA, 1988, pp. 235-44.
2. K. Harris, G.L. Erickson, and R.E. Schwer: *Proc. Conf. on High Temperature Alloys for Gas Turbines and Other Applications*, Liege, Belgium, Oct. 1986, D. Reidel Publishing Company, Dordrecht, Holland, 1986, pp. 709-18.
3. D.A. Ford and R.P. Arthery: *Superalloys 1984, Proc. Int. Symp. on Superalloys*, Seven Springs, Champion, PA, 1984, M. Gell, C.S. Kortovich, R.H. Bricknell, W.B. Kent, and J.F. Radvich, eds., TMS, Warrendale, PA, 1984, pp. 115-24.
4. T. Yamagata, H. Harata, S. Nagazawa, M. Yamazaki, and Y.G. Nakazawa: *Superalloys 1984, Proc. Int. Symp. on Superalloys*, Seven Springs, Champion, PA, 1984, M. Gell, C.S. Kortovich, R.H. Bricknell, W.B. Kent, and J.F. Radvich, eds., TMS, Warrendale, PA, 1984, pp. 157-66.
5. N. Yukawa, M. Morinaga, Y. Murata, H. Ezaki, and S. Inoue: *Superalloys 1988, Proc. Symp. on Superalloys*, Seven Springs, Champion, PA, 1988, D.N. Duhl, G. Maurer, S. Antolovich, C. Lund, and S. Reichman, eds., TMS, Warrendale, PA, 1988, pp. 225-34.
6. Y. Ohta, Y.G. Nakagawa, and S. Ohama: *Tetsu-to-Hagané*, 1990, vol. 76, pp. 940-47.
7. M. Morinaga, N. Yukawa, and H. Adachi: *J. Phys. Soc. Jpn.*, 1984, vol. 53, pp. 653-63.
8. M. Morinaga, N. Yukawa, and H. Ezaki: *Phil. Mag. A*, 1985, vol. 51, pp. 223-46.
9. M. Morinaga, N. Yukawa, and H. Ezaki: *Phil. Mag. A*, 1985, vol. 51, pp. 247-52.
10. N. Yukawa, M. Morinaga, H. Ezaki, and Y. Murata: *Proc. Conf. on High Temperature Alloys for Gas Turbines and Other Applications*, Oct. 1986, D. Reidel Publishing Company, Dordrecht, Holland, 1986, pp. 935-44.
11. K. Matsugi, R. Yokoyama, Y. Murata, M. Morinaga, and N. Yukawa: *Proc. Int. Conf. on High Temperature Materials for Power Engineering 1990*, C.R.M., Liege, Belgium, 1990, pp. 1251-60.

12. A.M. Beltran and D.A. Shores: *Superalloys*, C.T. Sims and W.C. Hagel, eds., A Wiley-Interscience Publication, 1972, p. 317.
13. G. Lom Bardi: *For Better Thermal Analysis*, 2nd ed., Istituto di Mineralogiae Petrografia Dell'universita di Roma, Citta Universitaria, Rome, Italy, 1980, pp. 24-25.
14. O.H. Kriege and J.M. Baris: *Trans. ASM*, 1967, vol. 62, pp. 195-203.
15. J.E. Restall and E.C. Joulson: *Met. Mater.*, vols. 134 and 187, 1973.
16. J.S. Zhang, Z.Q. Hu, Y. Murata, M. Morinaga, and N. Yukawa: *Metall. Trans. A*, 1993, vol. 24A, pp. 2451-64.
17. Decker: *Proc. of the Steel Strengthening Mechanisms Symp.*, Zurich, Switzerland, May 5–6, 1969, pp. 1-24.